SCIENCE CHINA
Information Sciences

• RESEARCH PAPER •

December 2019, Vol. 62 222202:1–222202:16
https://doi.org/10.1007/s11432-018-9844-3

Event-triggered attitude tracking for rigid spacecraft

Deheng CAI[1†], Hengguang ZOU[1,2†], Junzheng WANG[1], Yuan HUANG[1] & Dawei SHI[1*]

[1]*State Key Laboratory of Intelligent Control and Decision of Complex Systems, School of Automation, Beijing Institute of Technology, Beijing* 100081*, China;*
[2]*China Academy of Space Technology, Beijing* 100094*, China*

Received 9 October 2018/Revised 28 January 2019/Accepted 4 March 2019/Published online 12 November 2019

Abstract This study aims to investigate the problem of attitude control for a spacecraft with inertial uncertainties, external disturbances, and communication restrictions. An event-triggered active disturbance rejection control approach is proposed for attitude tracking of the spacecraft. An event-triggered mechanism is introduced together with an extended state observer to jointly monitor the system states and total disturbances. The observation error is proved to be uniformly bounded. Based on the proposed control scheme, the integrated tracking system is shown to be asymptotically stable, implying successful attitude tracking of the spacecraft for the desired motion. Numerical results illustrate the effectiveness of the control strategy in achieving satisfactory tracking performance with a reduced data-transmission cost.

Keywords spacecraft, attitude tracking, active disturbance rejection control, event-triggered control, extended state observer

Citation Cai D H, Zou H G, Wang J Z, et al. Event-triggered attitude tracking for rigid spacecraft. Sci China Inf Sci, 2019, 62(12): 222202, https://doi.org/10.1007/s11432-018-9844-3

1 Introduction

Control systems play an important role in achieving attitude maneuvering, attitude tracking, and high-precision pointing of spacecraft. Because the kinematic and dynamic equations of rigid spacecraft possess highly coupled nonlinear characteristics and systems may suffer from external disturbances, inertia-matrix uncertainties, and even actuator failures, the attitude-control problem has attracted significant attention over the past few decades [1–5].

A few strategies have been investigated for attitude-control problems of rigid spacecraft under different restrictive conditions, such as sliding mode control [6, 7], adaptive robust control [8, 9], and optimal control [10]. Considering the limitations of the onboard communication and computation resources for embedded computer systems on spacecraft, resource-aware control strategies should be investigated for attitude control. One feasible strategy for this is event-triggered control, wherein signals are only transmitted when the pre-designed event-triggering conditions are violated. In this regard, event-triggered control can reduce communication bandwidth and power to save more resources for other tasks, and also can increase the service lifetime of the entire system. Event-based sampling and control was originally introduced in [11] and has been applied in many control problems [12–15], including attitude control of the spacecraft [16–19]. In [16], an event-triggered control approach to reduce the control-updating frequency was proposed for spacecraft-attitude stabilization, but without considering the effect of disturbances. The same problem was addressed in [17], where two different types of triggering events, i.e.,

* Corresponding author (email: daweishi@bit.edu.cn)
† Cai D H and Zou H G have the same contribution to this work.

fixed- and relative-threshold strategies, were proposed. Attitude stabilization with an event-triggered mechanism and external disturbances was considered in [18]. In [19], an observer-based event-triggered control approach was proposed to cope with external disturbances and actuator faults and to reduce the control-updating frequency.

Unlike Refs. [16–19], which focused upon attitude stabilization, we investigated an event-triggered attitude-tracking problem for a spacecraft with inertial uncertainties and external disturbances. In particular, we reduced the transmission frequency of measurements of the states, rather than the control-updating frequency. Moreover, we considered the effect of inertial uncertainties that are coupled to the system states and make the attitude tracking more difficult to achieve with reduced sampling frequency. To attenuate these effects, we utilize an active disturbance rejection control (ADRC) approach to the control-system design. ADRC has shown its effectiveness in uncertainty and external disturbance rejection [20–22], and has been adopted in a wide range of applications [23–26]. The core of ADRC is to regard the internal uncertainties and external disturbances as a state of the system, which is the so-called extended state estimated by an extended state observer (ESO). Herein, to reduce the data-transmission rate, the ESO is integrated with the designed event-triggered mechanism. Some related investigations had been done by the authors' group [27, 28]. In [27], an event-triggered ESO (ET-ESO) was proposed, and the observation error was proved to be uniformly bounded. In [28], trajectory tracking of a DC torque motor was achieved based on the proposed event-triggered ADRC, where ET-ESO was utilized. Unlike Refs. [27, 28], a few challenges exist in the event-triggered attitude-tracking problem. First, the attitude kinematics and dynamics of a rigid spacecraft modeled by the unit quaternion technique possess highly coupled nonlinear characteristics; second, system dynamics including the gains of the inputs are strongly affected by external disturbances and inertial uncertainties, making the stabilization a nontrivial problem. Specifically, we focus on how to utilize ESO to observe the coupled three-channel disturbances and how to design an event-triggered mechanism to guarantee the stability of the integrated tracking system without information about the disturbances. The main contributions of this paper are summarized as follows.

(1) An event-triggered mechanism is proposed for attitude tracking of a spacecraft under communication-resource restrictions. The event-triggered mechanism only needs measurements of spacecraft-attitude orientation and angular velocity, without information concerning parameter uncertainties and external disturbances.

(2) Using the designed event-triggered mechanism, an event-triggered ADRC (ET-ADRC) scheme is proposed and the corresponding theoretical analysis is also developed. The asymptotic upper bounds on the steady-state-observation errors with parameters in the event-triggering condition are provided. Moreover, the tracking system is proved to be asymptotically stable, such that control of the spacecraft tracking the desired attitude motion is achieved based on the proposed scheme.

The developed results are validated by numerical simulations, which show that in comparision with the time-triggered ADRC scheme, the ET-ADRC scheme possesses satisfactory tracking performance at a reduced average data transmission rate. The remainder of this paper is organized as follows. In Section 2, the attitude-tracking system for a rigid spacecraft is described and the problem is formulated. The theoretical analysis of the performance of the event-triggered ADRC scheme is presented in Section 3. The simulation results are provided in Section 4, and Section 5 presents some concluding remarks.

Notation. $\mathbb{R}$ denotes the field of all real numbers. $\mathbb{R}^n$ denotes the n-dimensional real vector space. $\|\cdot\|$ and $|\cdot|$ denote the Euclidean norms of real vectors and the absolute values of scalars, respectively. I_n is the identity matrix of dimension n. a^{T} denotes the transposition of a. The shorthand $\mathrm{diag}\{b_1, b_2, \ldots, b_n\}$ denotes a diagonal matrix with diagonal blocks $b_1, b_2, \ldots, b_n$. The operator $a^{\times}$ denotes a skew-symmetric matrix of any vector $a = [a_1, a_2, a_3]^{\mathrm{T}}$ such that

$$a^{\times} = \begin{bmatrix} 0 & -a_3 & a_2 \\ a_3 & 0 & -a_1 \\ -a_2 & a_1 & 0 \end{bmatrix}.$$

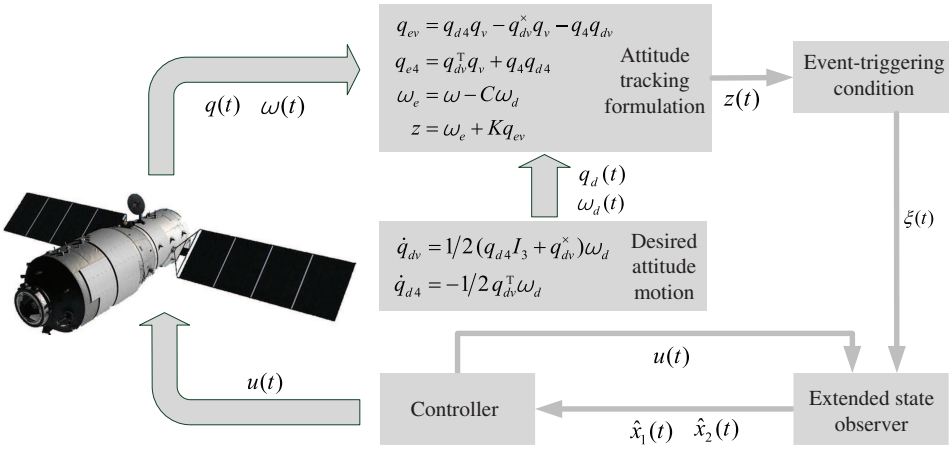

Figure 1 Schematic of the event-triggered ADRC scheme.

2 Problem formulation

Consider the event-triggered control scheme for attitude tracking in Figure 1. The attitude kinematics and dynamics of a rigid spacecraft can adequately be modeled as follows [1] in terms of the unit quaternion that is free of singularity:

$$\dot{q}_v = \frac{1}{2}(q_4 I_3 + q_v^{\times})\omega, \quad \dot{q}_4 = -\frac{1}{2}q_v^{\mathrm{T}}\omega, \quad J\dot{\omega} = -\omega^{\times}J\omega + u + d, \tag{1}$$

where $\omega \in \mathbb{R}^3$ is the angular velocity of the spacecraft; $u \in \mathbb{R}^3$ and $d \in \mathbb{R}^3$ are the control torques and external unknown disturbances, respectively; $J \in \mathbb{R}^{3\times 3}$ is the symmetric inertial matrix of the spacecraft; the unit quaternion $q = [q_v^{\mathrm{T}}, q_4]^{\mathrm{T}} \in \mathbb{R}^3 \times \mathbb{R}$ represents the attitude orientation of a body-fixed frame with respect to an inertial frame comprising a vector part $q_v = [q_1, q_2, q_3]^{\mathrm{T}} \in \mathbb{R}^3$ and scalar component $q_4 \in \mathbb{R}$, which satisfies the constraint $q_v^{\mathrm{T}}q_v + q_4^2 = 1$.

The attitude-tracking problem is formulated according to the related investigations [7,10]. The desired attitude motion is supposed to be generated by

$$\dot{q}_{dv} = \frac{1}{2}(q_{d4}I_3 + q_{dv}^{\times})\omega_d, \quad \dot{q}_{d4} = -\frac{1}{2}q_{dv}^{\mathrm{T}}\omega_d, \tag{2}$$

where $q_d = [q_{dv}^{\mathrm{T}}, q_{d4}]^{\mathrm{T}} \in \mathbb{R}^3 \times \mathbb{R}$ is the target-attitude unit quaternion satisfying $q_{dv}^{\mathrm{T}}q_{dv} + q_{d4}^2 = 1$; ω_d is the target angular velocity. Following the discussions in [10], ω_d, $\dot{\omega}_d$ and $\ddot{\omega}_d$ are assumed to be bounded. Subsequently, the objective of attitude tracking can be expressed as

$$\limsup_{t\to\infty} \eta_1(t) = 0, \quad \eta_1(t) = q(t) - q_d(t); \quad \limsup_{t\to\infty} \eta_2(t) = 0, \quad \eta_2(t) = \omega(t) - \omega_d(t). \tag{3}$$

This problem can be turned into the stabilization problem by considering the attitude-tracking-error quaternion $q_e = [q_{ev}^{\mathrm{T}}, q_{e4}]^{\mathrm{T}} \in \mathbb{R}^3 \times \mathbb{R}$ introduced in [1]

$$q_{ev} = q_{d4}q_v - q_{dv}^{\times}q_v - q_4 q_{dv}, \quad q_{e4} = q_{dv}^{\mathrm{T}}q_v + q_4 q_{d4}, \quad \omega_e = \omega - C\omega_d, \tag{4}$$

where $C = (1 - 2q_{ev}^{\mathrm{T}}q_{ev})I_3 + 2q_{ev}q_{ev}^{\mathrm{T}} - 2q_{e4}q_{ev}^{\times}$ with $\|C\| = 1$ and $\dot{C} = -\omega_e^{\times}C$; the error quaternion also satisfies the constraint $q_{ev}^{\mathrm{T}}q_{ev} + q_{e4}^2 = 1$ according to [10]. The attitude-tracking system can be formulated as follows:

$$\dot{q}_{ev} = \frac{1}{2}(q_{e4}I_3 + q_{ev}^{\times})\omega_e, \quad \dot{q}_{e4} = -\frac{1}{2}q_{ev}^{\mathrm{T}}\omega_e, \tag{5}$$

$$J\dot{\omega}_e = -(\omega_e + C\omega_d)^{\times}J(\omega_e + C\omega_d) + J(\omega_e^{\times}C\omega_d - C\dot{\omega}_d) + u + d. \tag{6}$$

For the purpose of the control-law design, Lemmas 1 and 2 are presented as follows.

Lemma 1. The objectives (3) can be achieved if there exists a control law for system (5) and (6) such that $\lim_{t\to\infty} q_{ev}(t) = 0$ and $\lim_{t\to\infty} \omega_e(t) = 0$.

Proof. This result can be proved based on analysis of sections II and III in [29].

Taking the coordinate transformation of $z = \omega_e + Kq_{ev}$ in [9], systems (5) and (6) can be rewritten as

$$\dot{q}_{ev} = \frac{1}{2}(q_{e4}I_3 + q_{ev}^{\times})\omega_e, \quad \dot{q}_{e4} = -\frac{1}{2}q_{ev}^{\mathrm{T}}\omega_e, \tag{7}$$

$$J\dot{z} = -(\omega_e + C\omega_d)^{\times}J(\omega_e + C\omega_d) + J(\omega_e^{\times}C\omega_d - C\dot{\omega}_d) + \frac{1}{2}JK(q_{e4}I_3 + q_{ev}^{\times})\omega_e + u + d, \tag{8}$$

where K is a positive definite matrix.

Lemma 2 ([7])**.** Consider the rigid spacecraft governed by systems (7) and (8). Then, for any $z(t)$ satisfying $\lim_{t\to\infty} z(t) = 0$, it follows that $\lim_{t\to\infty} q_{ev}(t) = 0$ and $\lim_{t\to\infty} \omega_e(t) = 0$, respectively.

Owing to the fuel consumption and payload variations, parameter uncertainties of the inertial matrix may exist in the control system. Similar to [7], the inertial matrix containing parameter uncertainties is in the form $J = J_0 + \Delta J$, where J_0 denotes the known nominal matrix that is selected to be nonsingular and ΔJ is the uncertainty associated with J. Thus, the dynamics given by (8) can be rewritten as

$$\begin{aligned}(J_0 + \Delta J)\dot{z} =& -(\omega_e + C\omega_d)^{\times}(J_0 + \Delta J)(\omega_e + C\omega_d) + (J_0 + \Delta J)(\omega_e^{\times}C\omega_d - C\dot{\omega}_d)\\ &+ \frac{1}{2}(J_0 + \Delta J)K(q_{e4}I_3 + q_{ev}^{\times})\omega_e + u + d.\end{aligned} \tag{9}$$

In fact, the disturbance forces caused by solar radiation, aerodynamics, and magnetic fields vary slowly in time, and the properties of the spacecraft (e.g., shape and mass) also vary slowly in time because of fuel consumption and payload variations. Therefore, reasonable assumptions are given out as follows.

Assumption 1. The disturbance d in (1) is assumed to be bounded as $\|d\| \leqslant D_1$ and to be differentiable with the bound, i.e., $\|\dot{d}\| \leqslant D_2$, where the D_1 and D_2, are unknown positive constants.

Assumption 2. The uncertainty part of the inertial matrix ΔJ is assumed to be bounded as $\|\Delta J\| \leqslant J_c$, where J_c is an unknown positive constant. The inertial matrix is assumed to be slowly varying, that is, $\|\dot{J}\| \leqslant J_d$ with J_d being an unknown positive constant.

As suggested in [7, 30, 31], these assumptions are quite common in the framework of robust attitude control of the rigid spacecraft.

On the other hand, utilizing the matrix inversion lemma, $(J_0 + \Delta J)^{-1}$ can be expressed as follows:

$$(J_0 + \Delta J)^{-1} = J_0^{-1} + \Delta\tilde{J}, \quad \text{with } \Delta\tilde{J} = -(I_3 + J_0^{-1}\Delta J)^{-1}J_0^{-1}\Delta J J_0^{-1},$$

where $\Delta\tilde{J}$ is an additive uncertainty. Then, following some simple algebraic transformations to (9), we obtain

$$\dot{z} = F + G + J_0^{-1}u + \bar{d}, \tag{10}$$

where

$$F = J_0^{-1}\left[-\omega^{\times}J_0\omega + J_0(\omega_e^{\times}C\omega_d - C\dot{\omega}_d) + \frac{1}{2}J_0K(q_{e4}I_3 + q_{ev}^{\times})\omega_e\right], \tag{11}$$

$$\begin{aligned}G =& J_0^{-1}\left[-\omega^{\times}\Delta J\omega + \Delta J(\omega_e^{\times}C\omega_d - C\dot{\omega}_d) + \frac{1}{2}\Delta JK(q_{e4}I_3 + q_{ev}^{\times})\omega_e\right]\\ &+ \Delta\tilde{J}\left[-\omega^{\times}J\omega + J(\omega_e^{\times}C\omega_d - C\dot{\omega}_d) + \frac{1}{2}JK(q_{e4}I_3 + q_{ev}^{\times})\right] + \Delta\tilde{J}u,\end{aligned} \tag{12}$$

$$\bar{d} = (J_0^{-1} + \Delta\tilde{J})d. \tag{13}$$

It is obvious that the attitude-tracking system in the presence of parameter uncertainties and unknown bounded disturbances has been modeled in (10). Finally, according to Lemmas 1 and 2, if there exists a dynamic state-feedback-control law for system (10) such that $\lim_{t\to\infty} z(t) = 0$, it follows that the

tracking objectives in (3) are achieved. Herein, we introduce ADRC to design one such control law. ADRC inherits a simple structure from proportional-integral-derivative (PID) that is error-driven rather than model-based and takes from modern control theory its best offering of the state observer [20]. The core of ADRC is to regard the disturbances including modeling errors as an additional state of the system, and then to compensate for them in the control law, which can be designed as a linear feedback or nonlinear feedback of the tracking errors. According to the original ESO formulation in [20, 32, 33], internal uncertainties and external disturbances can all be regarded as the "total disturbance", which is defined as an extended state. In this regard, we define the extended state x_2 as

$$x_2 = F + G + \bar{d}. \tag{14}$$

Furthermore, we write $x_1 := z$; then the system (10) can be written as

$$\dot{x}_1 = x_2 + J_0^{-1}u, \quad \dot{x}_2 = h(t), \tag{15}$$

where the function $h(t)$ is the derivative of the extended state assumed to satisfy Assumption 3.

Assumption 3. The derivative of the extended state is assumed to be bounded, namely, $|h_i(t)| \leqslant M_i$, where $i \in \{1, 2, 3\}$, and M_i are some nonnegative constants.

Remark 1. The extended state x_2 in (14) represents the total disturbances, which integrate the various information of disturbances, actual, desired angular velocities and attitude unit quaternions. Suppose Assumptions 1 and 2 hold; then, from (13), it is clear that $\dot{\bar{d}}$, the derivative of $\bar{d}$ is bounded. Note that the spacecraft is always under smooth operation, which implies that angular velocity ω and its derivative are bounded. ω_d, $\dot{\omega}_d$ and $\ddot{\omega}_d$ are the desired system states that are designed to be bounded. Furthermore, q_{ev}, q_{e4} and C and their derivatives are bounded due to $\|q_e\| = \|C\| = 1$. Then, according to (11), we can conclude that $\dot{F}$ is bounded. The control law u and its derivative can be designed to be bounded, and with the bounded conditions on $\dot{F}$ and $\dot{\bar{d}}$, we can conclude that $\dot{G}$ is bounded based on (12). By combining the discussions above, we find that the derivative of x_2 is bounded. Similar assumptions are also made in [34, 35]. Note that F includes additional uncertainties due to the asynchronous information caused by the event-triggered sampling scheme adopted herein. Consequently, we treat F as additional disturbances to be a part of the extended state in our design, which differs from [7].

Now we introduce the ET-ESO:

$$\begin{aligned}
\dot{\hat{x}}_1(t) &= \hat{x}_2(t) + g_1\left(\frac{1}{\varepsilon}[\xi(t) - \hat{x}_1(t)]\right) + J_0^{-1}u, \quad \hat{x}_1(t_0) = \hat{x}_{10},\\
\dot{\hat{x}}_2(t) &= \frac{1}{\varepsilon}g_2\left(\frac{1}{\varepsilon}[\xi(t) - \hat{x}_1(t)]\right), \quad \hat{x}_2(t_0) = \hat{x}_{20},
\end{aligned} \tag{16}$$

where the above observer contains three subobservers. The suffix i denotes the ith element of the vector state. $[\hat{x}_{1i}, \hat{x}_{2i}]^{\mathrm{T}} \in \mathbb{R}^2, i \in \{1, 2, 3\}$ is the state of the ith observer, $[\hat{x}_{1i0}, \hat{x}_{2i0}]^{\mathrm{T}} \in \mathbb{R}^2$ is the initial value of $[\hat{x}_{1i}, \hat{x}_{2i}]$, ε_i is the high-gain parameter of the ith observer and $\frac{1}{\varepsilon} = \mathrm{diag}\{\frac{1}{\varepsilon_1}, \frac{1}{\varepsilon_2}, \frac{1}{\varepsilon_3}\}$. The operators $g_j(a) \in \mathbb{R}^3$, $j \in \{1, 2\}$ on any vector $a = [a_1, a_2, a_3]^{\mathrm{T}} \in \mathbb{R}^3$ are defined as $g_j(a) = [g_{j1}(a_1), g_{j2}(a_2), g_{j3}(a_3)]^{\mathrm{T}}$, where the detailed expressions of $g_{ji}(\cdot)$ are discussed next. $\xi(t)$ denotes the previously received output x_1 which is given by

$$\xi(t) = \begin{cases} x_1(t_k), & \text{if } \Gamma(t) = 0,\\ x_1(t), & \text{otherwise,} \end{cases} \tag{17}$$

where $\Gamma(t)$ is the triggering condition to be presented next and t_k is the transmission instant determined by the event-triggering condition. The value of $\xi(t)$ will be updated only when $\Gamma(t) = 1$.

For the ith observer, $g_{1i}(\cdot)$ and $g_{2i}(\cdot)$ are selected as $g_{1i}(y_1) = b_i y_1 + \varphi(y_1)$ and $g_{2i}(y_1) = c_i y_1$ with

$\varphi(\theta)$ defined as follows:

$$\varphi(\theta)=\begin{cases}-\dfrac{1}{4}, & \theta<-\dfrac{\Pi}{2},\\ \dfrac{1}{4}\sin\theta, & -\dfrac{\Pi}{2}\leqslant\theta\leqslant\dfrac{\Pi}{2},\\ \dfrac{1}{4}, & \theta>\dfrac{\Pi}{2}.\end{cases}\tag{18}$$

Moreover, b_i and c_i are some constants such that the matrix $A:=\left[\begin{smallmatrix}-b_i & 1\\ -c_i & 0\end{smallmatrix}\right]$ is Hurwitz; then there exists a matrix $\tilde{P}>0$ satisfying

$$\tilde{P}A+A^{\mathrm{T}}\tilde{P}=-I.\tag{19}$$

We define functions $P_i:\mathbb{R}^2\to\mathbb{R}$ as $P_i(y)=\langle\tilde{P}y,y\rangle+\int_0^{y_1}\varphi(s)\mathrm{d}s$. By choosing the functions $g_{1i},\ g_{2i}$, and φ in this form with b_i and c_i satisfying the inequality of $(1+c_i)/b_i+b_i<4$, which are discussed in the supplementary document of [36], there exist nonnegative-definite functions $\Theta_i:\mathbb{R}^2\to\mathbb{R}$ such that

$$\lambda_{1i}\|y\|^2\leqslant P_i(y)\leqslant\lambda_{2i}\|y\|^2,\tag{20}$$

$$\lambda_{3i}\|y\|^2\leqslant\Theta_i(y)\leqslant\lambda_{4i}\|y\|^2,\tag{21}$$

$$\frac{\partial P_i}{\partial y_1}(y_2-g_{1i}(y_1))-\frac{\partial P_i}{\partial y_2}g_{2i}(y_1)\leqslant-\Theta_i(y),\tag{22}$$

$$\left\|\frac{\partial P_i}{\partial y}\right\|\leqslant\tau_i\|y\|,\tag{23}$$

where $\lambda_{1i},\ \lambda_{2i},\ \lambda_{3i},\ \lambda_{4i}$, and τ_i are some positive constants. The minimum and maximum values of the corresponding parameters of the three subobservers are denoted with the suffixes min and max, respectively, e.g., $\{\lambda_{1i}\}$ with $\lambda_{1\min}$ and $\lambda_{1\max}$. The choice of $\varphi(\theta)$ is not unique as long as it satisfies the requirements above.

With the disturbances estimated by the ET-ESO, a dynamic state-feedback control law is designed as

$$u=-J_0\tilde{K}\hat{x}_1-J_0\hat{x}_2,\tag{24}$$

where $\tilde{K}=\mathrm{diag}\{\tilde{K}_1,\tilde{K}_2,\tilde{K}_3\}$, and $\tilde{K}_i$ are some positive constants.

For convenience of analysis, we define $\tilde{x}_j$, e_j and $\tilde{e}_i$ as

$$\begin{aligned}&\tilde{x}_j:=x_j-\hat{x}_j,\quad e_j:=[e_{j1},e_{j2},e_{j3}]^{\mathrm{T}}=\left[\frac{\tilde{x}_{j1}}{\varepsilon_1^{2-j}},\frac{\tilde{x}_{j2}}{\varepsilon_2^{2-j}},\frac{\tilde{x}_{j3}}{\varepsilon_3^{2-j}}\right]^{\mathrm{T}},\quad j\in\{1,2\},\\ &\tilde{e}_i:=[e_{1i},e_{2i}]^{\mathrm{T}},\quad i\in\{1,2,3\},\end{aligned}\tag{25}$$

where the $\tilde{e}_i$ is related to the observation error of the ith observer consisting of the ith element of e_1 and e_2. We define the sampling error $\sigma(t)$ as $\sigma(t):=\frac{1}{\varepsilon}[x_1(t_k)-x_1(t)]$, $t\in[t_k,t_{k+1})$ and, for notional brevity, we define $\alpha_j(e_1,\sigma)$ as $\alpha_j(e_1,\sigma):=g_j(e_1+\sigma)-g_j(e_1),\ j\in\{1,2\}$.

In this work, we consider the following problems:

(1) Is there an event-triggering condition such that the observation errors' boundedness of three subobservers can be guaranteed?

(2) Based on the proposed event-triggering condition and the designed control law, can we stabilize the system (10) in the presence of inertial uncertainties and unknown disturbances?

3 Main results

Herein, the problems outlined in the previous section are investigated. The control law u in (24) can also be expressed as

$$u=-J_0\tilde{K}x_1+J_0\tilde{K}(x_1-\hat{x}_1)-J_0\hat{x}_2=-J_0\tilde{K}x_1+J_0\tilde{K}\varepsilon e_1-J_0\hat{x}_2,\tag{26}$$

where $\varepsilon = \mathrm{diag}\{\varepsilon_1, \varepsilon_2, \varepsilon_3\}$. The minimum and maximum values of $\{\varepsilon_i\}$ are denoted as $\varepsilon_{\min}$ and $\varepsilon_{\max}$, respectively. An event-triggering condition of the observer is proposed to have the following form:

$$\Gamma(t) = \begin{cases} 0, & \text{if } \sum_{i=1}^{3}\sum_{j=1}^{2} |\alpha_{ji}(e_{1i}, \sigma_i)| \leqslant \Psi\varepsilon_{\min}, \\ 1, & \text{otherwise}, \end{cases} \tag{27}$$

where $\alpha_{ji}(\cdot)$ is the ith component of vector $\alpha_j(\cdot)$ and Ψ is a given constant. Now, we are ready to analyze the performance of the proposed event-triggered control scheme in Theorem 1.

Theorem 1. Consider the closed-loop system in (7) and (8), the ESO in (16), and the control law in (24). Suppose that Assumptions 1–3 hold. For any initial values of x_1, x_2 and $\hat{x}_1$, $\hat{x}_2$, and a given $\Psi > 0$, there exist $\varepsilon^* > 0$ and an event-triggering condition in (27) of the observer such that for any $\varepsilon_i \in (0, \varepsilon^*)$, $i \in \{1, 2, 3\}$, it holds that, for $j \in \{1, 2\}$,

$$\limsup_{t\to\infty} \|x_j - \hat{x}_j\| \leqslant \varepsilon_{\max}^{2-j} \sqrt{\frac{3\varepsilon_{\max}^{\frac{1}{2}}}{2\gamma\lambda_{1\min}}[(\tau M)_{\max} + (\tau\Psi)_{\max}]}, \tag{28}$$

$$\limsup_{t\to\infty} \|z\| \leqslant \sqrt{\frac{3\varepsilon_{\max}^{\frac{1}{2}}}{\gamma}[(\tau M)_{\max} + (\tau\Psi)_{\max}]}, \tag{29}$$

where $(\tau M)_{\max}$ and $(\tau\Psi)_{\max}$ are the maximum values of $\{\tau_i M_i\}$ and $\{\tau_i\Psi\}$, $i \in \{1, 2, 3\}$, respectively.

Proof. From (15), (16) and the definitions of $\tilde{x}_j$ and e_j in (25), we find that

$$\begin{aligned} \dot{\tilde{x}}_1 &= x_2 - \hat{x}_2 - g_1\left(\frac{1}{\varepsilon}[\xi(t) - \hat{x}_1(t)]\right) \\ &= \tilde{x}_2 - g_1\left(\frac{1}{\varepsilon}[x_1(t) - \hat{x}_1(t)] + \frac{1}{\varepsilon}[\xi(t) - x_1(t)]\right) = \tilde{x}_2 - g_1(e_1(t)) - \alpha_1(e_1(t), \sigma(t)), \\ \dot{\tilde{x}}_2 &= h(t) - g_2\left(\frac{1}{\varepsilon}[\xi(t) - \hat{x}_1(t)]\right) = h(t) - \frac{1}{\varepsilon}g_2(e_1(t)) - \frac{1}{\varepsilon}\alpha_2(e_1(t), \sigma(t)). \end{aligned}$$

Then, through a simple computation, we obtain the dynamics of e_j as

$$\begin{aligned} \dot{e}_1(t) &= \frac{1}{\varepsilon}e_2(t) - \frac{1}{\varepsilon}g_1(e_1(t)) - \frac{1}{\varepsilon}\alpha_1(e_1(t), \sigma(t)), \\ \dot{e}_2(t) &= h(t) - \frac{1}{\varepsilon}g_2(e_1(t)) - \frac{1}{\varepsilon}\alpha_2(e_1(t), \sigma(t)). \end{aligned} \tag{30}$$

Consider a nonnegative-definite function $V(x_1, e_1, e_2)$ as

$$V(x_1, e_1, e_2) = \frac{1}{2}x_1^{\mathrm{T}}x_1 + \sum_{i=1}^{3} P_i(\tilde{e}_i), \tag{31}$$

where $P_i(\tilde{e}_i)$ and $\tilde{e}_i$ are provided in (1) and (25), respectively. From the dynamics of e_j in (30), we observe through a simple computation that

$$\begin{aligned} \frac{\mathrm{d}V}{\mathrm{d}t} &= x_1^{\mathrm{T}}\dot{x}_1 + \sum_{i=1}^{3}\frac{\partial P_i}{\partial e_{1i}}\dot{e}_{1i} + \sum_{i=1}^{3}\frac{\partial P_i}{\partial e_{2i}}\dot{e}_{2i} \\ &= x_1^{\mathrm{T}}\dot{x}_1 + \sum_{i=1}^{3}\frac{\partial P_i}{\partial e_{1i}}\left[\frac{1}{\varepsilon_i}e_{2i}(t) - \frac{1}{\varepsilon_i}g_{1i}(e_{1i}(t)) - \frac{1}{\varepsilon_i}\alpha_{1i}(e_{1i}(t), \sigma_i(t))\right] \\ &\quad + \sum_{i=1}^{3}\frac{\partial P_i}{\partial e_{2i}}\left[h_i(t) - \frac{1}{\varepsilon_i}g_{2i}(e_{1i}(t)) - \frac{1}{\varepsilon_i}\alpha_{2i}(e_{1i}(t), \sigma_i(t))\right] \\ &\leqslant x_1^{\mathrm{T}}\dot{x}_1 + \sum_{i=1}^{3}\left|\frac{\partial P_i}{\partial e_{2i}}\right| |h_i(t)| + \sum_{i=1}^{3}\frac{1}{\varepsilon_i}\left[\frac{\partial P_i}{\partial e_{1i}}(e_{2i} - g_{1i}(e_{1i})) - \frac{\partial P_i}{\partial e_{2i}}g_{2i}(e_{1i})\right] \end{aligned}$$

$$-\sum_{i=1}^{3}\frac{1}{\varepsilon_i}\left[\frac{\partial P_i}{\partial e_{1i}}\alpha_{1i}(e_{1i},\sigma_i)+\frac{\partial P_i}{\partial e_{2i}}\alpha_{2i}(e_{1i},\sigma_i)\right]. \tag{32}$$

According to (15) and control law u in (26), we have

$$\begin{aligned}x_1^{\mathrm{T}}\dot{x}_1 &= x_1^{\mathrm{T}}[x_2-\tilde{K}x_1+\tilde{K}(x_1-\hat{x}_1)-\hat{x}_2]=x_1^{\mathrm{T}}(-\tilde{K}x_1+\tilde{K}\varepsilon e_1+e_2)\\ &\leqslant -\tilde{K}_{\min}\|x_1\|^2+\tilde{K}_{\max}\varepsilon_{\max}\|x_1\|\|e_1\|+\|x_1\|\|e_2\|\\ &\leqslant -\tilde{K}_{\min}\|x_1\|^2+\frac{1}{2}\left(\tilde{K}_{\max}^2\varepsilon_{\max}^{\frac{5}{2}}\|x_1\|^2+\varepsilon_{\max}^{-\frac{1}{2}}\|e_1\|^2\right)+\frac{1}{2}\left(\varepsilon_{\max}^{\frac{1}{2}}\|x_1\|^2+\varepsilon_{\max}^{-\frac{1}{2}}\|e_2\|^2\right).\end{aligned} \tag{33}$$

Considering the properties of functions $P_i(\cdot)$ and $\Theta_i(\cdot)$ in (21) and (22), we find that

$$\begin{aligned}\sum_{i=1}^{3}\frac{1}{\varepsilon_i}\left[\frac{\partial P_i}{\partial e_{1i}}(e_{2i}-g_{1i}(e_{1i}))-\frac{\partial P_i}{\partial e_{2i}}g_{2i}(e_{1i})\right] &\leqslant -\sum_{i=1}^{3}\frac{1}{\varepsilon_i}\Theta(\tilde{e}_i)\leqslant -\sum_{i=1}^{3}\frac{\lambda_{3i}}{\varepsilon_i}\|\tilde{e}_i\|^2\\ &\leqslant -\frac{\lambda_{3\min}}{\varepsilon_{\max}}(\|e_1\|^2+\|e_2\|^2).\end{aligned} \tag{34}$$

According to (23) and the event-triggering condition in (27), we observe that

$$\begin{aligned}&-\sum_{i=1}^{3}\frac{1}{\varepsilon_i}\left[\frac{\partial P_i}{\partial e_{1i}}\alpha_{1i}(e_{1i},\sigma_i)+\frac{\partial P_i}{\partial e_{2i}}\alpha_{2i}(e_{1i},\sigma_i)\right]\leqslant\sum_{i=1}^{3}\frac{1}{\varepsilon_i}\left[\left|\frac{\partial P_i}{\partial e_{1i}}\alpha_{1i}(e_{1i},\sigma_i)\right|+\left|\frac{\partial P_i}{\partial e_{2i}}\alpha_{2i}(e_{1i},\sigma_i)\right|\right]\\ &\leqslant\sum_{i=1}^{3}\frac{1}{\varepsilon_i}\tau_i\|\tilde{e}_i\|\Psi\varepsilon_i\leqslant\sum_{i=1}^{3}\frac{\tau_i\Psi}{2}\left(\varepsilon_{\max}^{-\frac{1}{2}}\|\tilde{e}_i\|^2+\varepsilon_{\max}^{\frac{1}{2}}\right)\leqslant\frac{(\tau\Psi)_{\max}}{2}\left(\varepsilon_{\max}^{-\frac{1}{2}}\|e_1\|^2+\varepsilon_{\max}^{-\frac{1}{2}}\|e_2\|^2+3\varepsilon_{\max}^{\frac{1}{2}}\right).\end{aligned} \tag{35}$$

Similarly, according to Assumption 3, we obtain that

$$\begin{aligned}\sum_{i=1}^{3}\left|\frac{\partial P_i}{\partial e_{2i}}\right||h_i(t)|&\leqslant\sum_{i=1}^{3}\tau_i\|\tilde{e}_i\|M_i\leqslant\sum_{i=1}^{3}\frac{\tau_iM_i}{2}\left(\varepsilon_{\max}^{-\frac{1}{2}}\|\tilde{e}_i\|^2+\varepsilon_{\max}^{\frac{1}{2}}\right)\\ &\leqslant\frac{(\tau M)_{\max}}{2}\left(\varepsilon_{\max}^{-\frac{1}{2}}\|e_1\|^2+\varepsilon_{\max}^{-\frac{1}{2}}\|e_2\|^2+3\varepsilon_{\max}^{\frac{1}{2}}\right).\end{aligned} \tag{36}$$

Combining the results (30)–(36), we finally obtain

$$\begin{aligned}\frac{\mathrm{d}V}{\mathrm{d}t}\leqslant&-\frac{1}{\varepsilon_{\max}}\left[\lambda_{3\min}-\frac{(\tau M)_{\max}+(\tau\Psi)_{\max}}{2}\varepsilon_{\max}^{\frac{1}{2}}-\frac{1}{2}\varepsilon_{\max}^{\frac{1}{2}}\right](\|e_1\|^2+\|e_2\|^2)\\ &-\left(\tilde{K}_{\min}-\frac{1}{2}\varepsilon_{\max}^{\frac{1}{2}}-\frac{\tilde{K}_{\max}^2}{2}\varepsilon_{\max}^{\frac{5}{2}}\right)\|x_1\|^2+\frac{3}{2}\varepsilon_{\max}^{\frac{1}{2}}[(\tau M)_{\max}+(\tau\Psi)_{\max}].\end{aligned}$$

We write

$$\begin{aligned}\beta_1&:=\tilde{K}_{\min}-\frac{1}{2}\varepsilon_{\max}^{\frac{1}{2}}-\frac{\tilde{K}_{\max}^2}{2}\varepsilon_{\max}^{\frac{5}{2}},\\ \beta_2&:=\lambda_{3\min}-\frac{(\tau M)_{\max}+(\tau\Psi)_{\max}}{2}\varepsilon_{\max}^{\frac{1}{2}}-\frac{1}{2}\varepsilon_{\max}^{\frac{1}{2}},\end{aligned} \tag{37}$$

and define ε^* as

$$\varepsilon^*=\max\{\varepsilon_{\max}\in\mathbb{R}|\beta_1\geqslant 0,\ \beta_2\geqslant 0,\ \text{and}\ \varepsilon_{\max}>0\}. \tag{38}$$

It is obvious that β_1 and β_2 are monotonically decreasing functions of $\varepsilon_{\max}$, that $\lim_{\varepsilon_{\max}\to 0}\beta_1>0$, $\lim_{\varepsilon_{\max}\to 0}\beta_2>0$, and that $\beta_1<0$, $\beta_2<0$ when $\varepsilon_{\max}$ becomes sufficiently large. Thus, ε^* is well defined. For $\varepsilon_{\max}\in(0,\varepsilon^*)$, we have

$$\frac{\mathrm{d}V}{\mathrm{d}t}\leqslant-\beta_1\|x_1\|^2-\frac{\beta_2}{\varepsilon_{\max}}(\|\tilde{e}_1\|^2+\|\tilde{e}_2\|^2+\|\tilde{e}_3\|^2)+\frac{3}{2}\varepsilon_{\max}^{\frac{1}{2}}[(\tau M)_{\max}+(\tau\Psi)_{\max}]$$

$$\leqslant -2\beta_1\frac{1}{2}x_1^{\mathrm{T}}x_1 - \frac{\beta_2}{\varepsilon_{\max}\lambda_{2\min}}\sum_{i=1}^{3}P_i(\tilde{e}_i) + \frac{3}{2}\varepsilon_{\max}^{\frac{1}{2}}[(\tau M)_{\max} + (\tau\Psi)_{\max}].$$

Furthermore, we define

$$\gamma := \min\left\{2\beta_1, \frac{\beta_2}{\varepsilon_{\max}\lambda_{2\min}}\right\}, \quad \phi(t,t_0) := \exp(-\gamma(t-t_0)), \tag{39}$$

and then $\frac{\mathrm{d}V}{\mathrm{d}t}$ can be rewritten as

$$\frac{\mathrm{d}V}{\mathrm{d}t} \leqslant -\gamma V + \frac{3}{2}\varepsilon_{\max}^{\frac{1}{2}}[(\tau M)_{\max} + (\tau\Psi)_{\max}]. \tag{40}$$

From (31), it is clear that $V \geqslant 0$, and then according to a comparison lemma in [37], we obtain that

$$V(x_1(t), e_1(t), e_2(t)) \leqslant W(t), \tag{41}$$

where $W(t)$ is the solution of the differential equation

$$\dot{W} = -\gamma W + \frac{3}{2}\varepsilon_{\max}^{\frac{1}{2}}[(\tau M)_{\max} + (\tau\Psi)_{\max}], \quad W(t_0) = V(x_1(t_0), e_1(t_0), e_2(t_0)). \tag{42}$$

Solving the differential equation in (42), we have

$$W(t) = V(x_1(t_0), e_1(t_0), e_2(t_0))\phi(t,t_0) + \frac{3}{2}\varepsilon_{\max}^{\frac{1}{2}}[(\tau M)_{\max} + (\tau\Psi)_{\max}]\int_{t_0}^{t}\phi(t,\nu)\mathrm{d}\nu. \tag{43}$$

Then, we obtain

$$\begin{aligned} V(x_1(t), e_1(t), e_2(t)) &\leqslant W(t) \\ &\leqslant V(x_1(t_0), e_1(t_0), e_2(t_0))\phi(t,t_0) + \frac{3}{2\gamma}\varepsilon_{\max}^{\frac{1}{2}}[(\tau M)_{\max} + (\tau\Psi)_{\max}](1-\phi(t,t_0)). \end{aligned}$$

Because $\phi(t,t_0) \to 0$ when $t \to \infty$, we have that when $t \to \infty$

$$V(x_1, e_1, e_2) \leqslant \frac{3}{2\gamma}\varepsilon_{\max}^{\frac{1}{2}}[(\tau M)_{\max} + (\tau\Psi)_{\max}]. \tag{44}$$

Using the fact in (20), when $t \to 0$ we find that

$$\frac{1}{2}\|x_1\| + \lambda_{1\min}(\|e_1\|^2 + \|e_2\|^2) \leqslant V(x_1, e_1, e_2). \tag{45}$$

From (44) and (45), we observe that

$$\limsup_{t\to\infty}\|z\| = \limsup_{t\to\infty}\|x_1\| \leqslant \sqrt{\frac{3\varepsilon_{\max}^{\frac{1}{2}}}{\gamma}[(\tau M)_{\max} + (\tau\Psi)_{\max}]}. \tag{46}$$

Similarly, we obtain that, for $j \in \{1,2\}$

$$\limsup_{t\to\infty}\|e_j\| \leqslant \sqrt{\frac{3\varepsilon_{\max}^{\frac{1}{2}}}{2\gamma\lambda_{1\min}}[(\tau M)_{\max} + (\tau\Psi)_{\max}]}, \tag{47}$$

and from the definitions of e_j, that

$$\limsup_{t\to\infty}\|x_j - \hat{x}_j\| \leqslant \varepsilon_{\max}^{2-j}\sqrt{\frac{3\varepsilon_{\max}^{\frac{1}{2}}}{2\gamma\lambda_{1\min}}[(\tau M)_{\max} + (\tau\Psi)_{\max}]}. \tag{48}$$

This completes the proof.

Remark 2. The ESO in (16), the control law in (24), and the event-triggering mechanism proposed in (27) can guarantee the asymptotic boundedness of the observation error and stabilize the system (10). According to Lemmas 1 and 2, the stability of system (10) implies that the states of the rigid spacecraft system governed by (1) can track the given desired attitudinal motion (2) in the presence of parameter uncertainties and unknown disturbances. Moreover, from (46) and (48), the system state z and observation errors can converge to an arbitrarily small bounded range around zero for properly chosen values of $\{\varepsilon_i\}$ and Ψ, even though the bound of the derivative of the extended state is unknown. The input-to-state stability of the ith ESO is ensured by the parameterization of the functions g_{ji}, $j \in \{1, 2\}$, and $\varphi(\theta)$, as chosen in Section 2, which satisfy the requirements in (19) and (20)–(23). The function $\varphi(\theta)$ is the nonlinear part of the ESO. The proposed event-triggering condition in (27) is related to the value of the sampling errors $\sigma(t)$ and Ψ. Only when $\sigma(t)$ becomes sufficiently large will the value of $\xi(t)$ be updated, so that the data-transmission cost is reduced. The transmission cost decreases with the increase of Ψ and vise versa. Furthermore, the system performance can also be adjusted by changing the value of parameter Ψ according to the quantitative relations in (46) and (48).

4 Numerical example

In this section, the effectiveness of the introduced event-triggered control scheme is evaluated by numerical simulations. Consider the nominal inertia matrix of the spacecraft model (1) of the following form [7]:

$$J_0 = \begin{bmatrix} 20 & 1.2 & 0.9 \\ 1.2 & 17 & 1.4 \\ 0.9 & 1.4 & 15 \end{bmatrix} \text{kg} \cdot \text{m}^2. \tag{49}$$

Moreover, parameter uncertainties of the inertial matrix are described as $\Delta J = \text{diag}[\sin(0.1t), 2\sin(0.2t), 3\sin(0.3t)]$ $\text{kg} \cdot \text{m}^2$. The external disturbances are described as $d(t) = [0.1\sin(0.1t), 0.2\sin(0.2t), 0.3\sin(0.2t)]^{\text{T}}$ $\text{N} \cdot \text{m}$. We performed two groups of simulations with different desired angular velocities, having sinusoid and square wave forms, respectively. The corresponding desired unit quaternion to be tracked is generated by (5).

Furthermore, all the initial values of the parameters in the two groups stay the same. The initial attitude orientation of the unit quaternion is $q(0) = [0.3, -0.2, -0.3, 0.8832]^{\text{T}}$, and the initial target unit quaternion is $q_d(0) = [0, 0, 0, 1]^{\text{T}}$. The initial value of the angular velocity is $\omega(0) = [0, 0, 0]^{\text{T}}$ rad/s.

For comparison purpose, in addition to the ET-ADRC controller, a time-triggered continuous-time ADRC (CT-ADRC) controller is also implemented for each group. In these simulations, the ADRC controllers are implemented by difference approximation with a sampling time $t_s = 0.001$ s. To evaluate the tracking performance of the system, we define the tracking errors of the angular velocity (E_v), unit quaternion (E_q), and average sampling time (T_A) as follows:

$$E_v = \frac{1}{3T}\int_0^T \sum_{i=1}^{3} |\omega_i - \omega_{di}| \text{d}t, \quad E_q = \frac{1}{4T}\int_0^T \sum_{i=1}^{4} |q_i - q_{di}| \text{d}t, \tag{50}$$

$$T_A = \begin{cases} 10, & \text{for CT-ADRC scheme,} \\ \dfrac{T}{N_s}, & \text{for ET-ADRC scheme,} \end{cases} \tag{51}$$

where we recall that the suffix d represents the desired target state, the suffix i denotes the ith element of the vector state, T is the total simulation time in milliseconds, and N_s is the total triggering counts in one simulation. Moreover, because energy consumption in attitude control is an extremely important fact to consider, comparison of energy consumption between the time- and event-triggered approaches is performed based on the energy-consumption model in [38] as follows:

$$E_c = \sum_{k=1}^{N}\sum_{i=1}^{3} \left| \frac{1}{2}\omega_i^2(k) - \frac{1}{2}\omega_i^2(k-1) \right|, \tag{52}$$

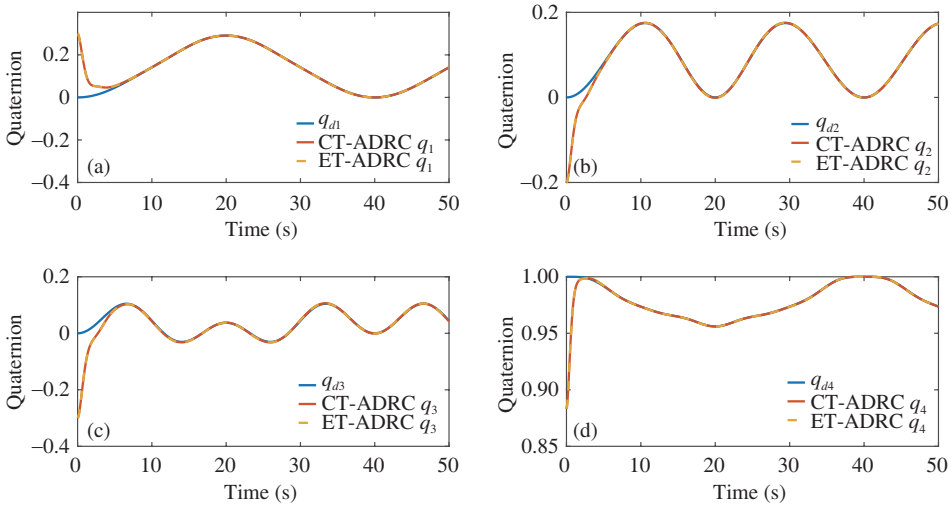

Figure 2 (Color online) Attitude quaternion tracking performance of sinusoidal form. Tracking performance for (a) q_1, (b) q_2, (c) q_3, and (d) q_4.

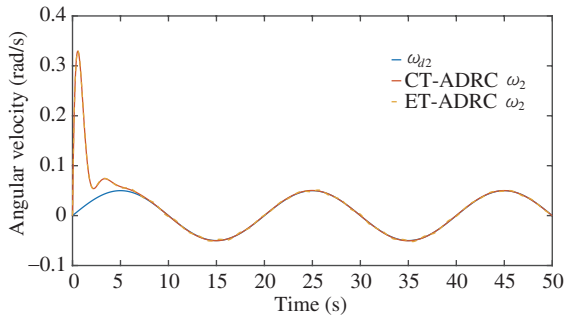

Figure 3 (Color online) Angular-velocity-tracking performance of sinusoidal form.

where $\omega_i(k)$ is the ith angular velocity at step k, and N denotes the total number of time steps in the whole simulation. Note that the difference here is that the mass of the spacecraft is not considered as it does not affect the comparison.

4.1 Desired angular velocity in sinusoidal form

The attitude-tracking problem for a spacecraft with the desired angular velocity in sinusoidal form is simulated in this subsection. The desired angular velocity is supposed to have the form

$$\omega_d(t) = 0.05\left[\sin\left(\frac{\pi t}{20}\right), \sin\left(\frac{2\pi t}{20}\right), \sin\left(\frac{3\pi t}{20}\right)\right]^{\mathrm{T}} \ \text{rad/s}. \tag{53}$$

Without loss of generality, the parameters of three sub-ESOs in (16) are selected to be the same, such that for any $i \in \{1,2,3\}$, $g_{1i}(y_1) = 2y_1 + \varphi(y_1)$ and $g_{2i}(y_1) = y_1$. The high-gain parameters are chosen as $\varepsilon_1 = \varepsilon_2 = \varepsilon_3 = 0.4$. The parameters K in (8) and $\tilde{K}$ in (24) are chosen as $K = 2I_3$ and $\tilde{K} = 4I_3$, respectively.

In particular, we performed the simulations considering the utilization of sampling periods equal to 1 and 400 ms for the time-triggered cases, and the utilization of event-triggering parameters, Ψ, that lead to different average sampling periods, i.e., 60.9 and 402 ms, for the event-triggered cases. The tracking results of the attitude quaternion and the angular-velocity component for the CT-ADRC scheme with 1-ms sampling periods and the ET-ADRC scheme with $\Psi = 0.1$ are shown in Figures 2 and 3, respectively. Moreover, the corresponding performances of the ESO observing states x_1 and x_2 for both schemes are shown in Figures 4 and 5, respectively. The tracking errors E_v, E_q, average sampling time

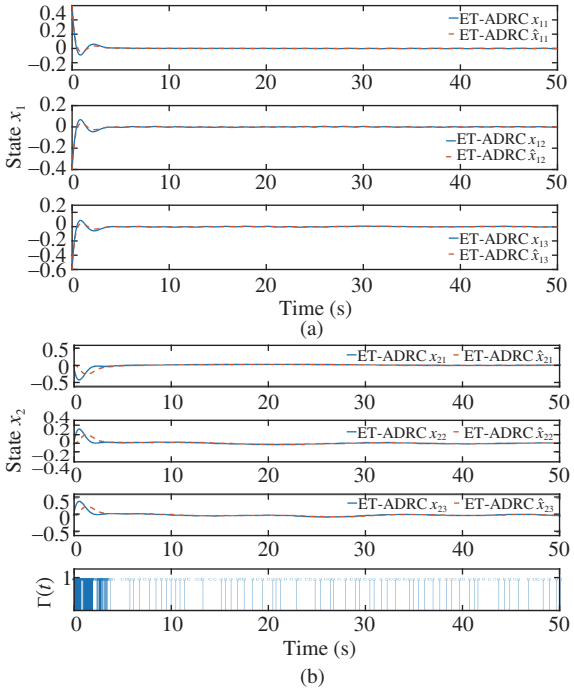

Figure 4 (Color online) Observation performance of ESO with event-triggered mechanism of sinusoidal form. Observation performance for (a) x_1 and (b) x_2.

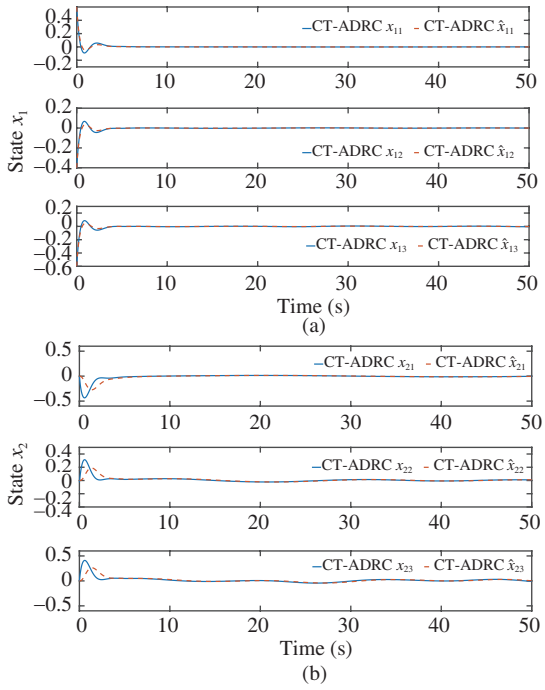

Figure 5 (Color online) Observation performance of ESO with time-triggered mechanism of sinusoidal form. Observation performance for (a) x_1 and (b) x_2.

Table 1 Performances of two control schemes of sinusoidal form

Simulation scheme	Average sampling time T_A (ms)	Tracking errors E_v/E_q	QEC E_c
Time-triggered	1	0.0115/0.0059	0.58
	400	0.0407/0.0073	3.41
Event-triggered	101.21 ($\Psi = 0.1$)	0.0122/0.0059	0.59
	402.13 ($\Psi = 1.5$)	0.0268/0.0075	0.84

T_A, and qualitative energy consumption (QEC) E_c are summarized in Table 1. From Table 1, we observe that, in comparison with a small sampling period (1 ms) for time-triggered control, the proposed scheme can maintain a comparable control performance and almost identical energy consumption (achieved by a time-triggered controller with a high sampling frequency) at a much smaller average sampling rate. Moreover, we also observe that when the (average) sampling periods are both increased to larger values (approximately 400 ms), the proposed scheme leads to a much smaller energy consumption index. The implication is that ET-ADRC scheme is more energy-efficient in certain extreme cases (e.g., sensor faults or communication bandwidth outrage) and bears improved fault-tolerant robustness in terms of performance and energy efficiency. Additionally, the results of sampling intervals between two consecutive event-triggering instants are provided in Figure 6, where we can observe that nonzero sampling intervals can be guaranteed to avoid Zeno behavior. With longer inter-triggering intervals, the cost of data transmission and computation can be reduced.

For the ET-ADRC scheme with $\Psi = 0.1$, we perform comparative analysis concering the effects of uncertainties in terms of tracking errors and average input signal. In particular, the uncertainties considered in the simulations include the external disturbances and parameter uncertainties of the inertial matrix. The results are presented in Table 2; we observe that the ET-ADRC scheme with uncertainties has similar tracking performance in terms of tracking errors but requires larger inputs in comparison with the cases without uncertainties. This is because of the disturbance-rejection capability of ADRC. Thus, the ET-ADRC scheme is required to produce larger input signals to eliminate the effects of

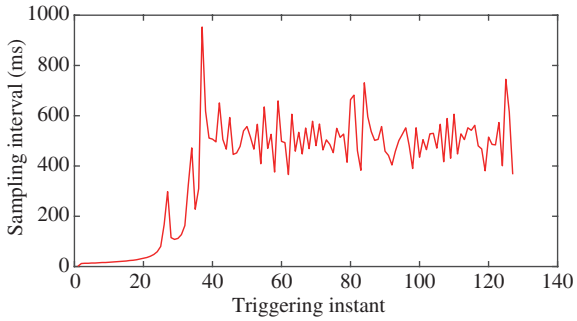

Figure 6 (Color online) Sampling intervals of ET-ADRC scheme with $\Psi = 1.5$ for sinusoidal form.

Table 2 The effect of uncertainties upon the performance of the ET-ADRC scheme with $\Psi = 0.1$

Reference	Simulation scenario	Average inputs signal (N*m)	Tracking errors E_v/E_q
Sinusoid form	With uncertainties	1.49	0.0122/0.0059
	Without uncertainties	1.35	0.0123/0.0059
Squarewave form	With uncertainties	1.90	0.0158/0.0063
	Without uncertainties	1.67	0.0157/0.0063

Table 3 Performances of two control schemes of square wave form

Simulation scheme	Average sampling time T_A (ms)	Tracking errors E_v/E_q	QEC E_c
Time-triggered	1	0.0152/0.0063	0.60
	400	0.0575/0.0094	3.77
Event-triggered	60.90 ($\Psi = 0.1$)	0.0158/0.0063	0.61
	401.52 ($\Psi = 2.5$)	0.0402/0.0092	1.16

uncertainties.

The performance of the system largely relies on the selection of parameters, especially the parameters $\tilde{K}$ of the control law, ε_i and Ψ of the sub-ESOs, and event-triggered mechanism. Larger Ψ can reduce resource consumption with lower average sampling rates but the observation errors are more likely to be bigger, causing larger tracking errors. A smaller ε_i can speed up the convergence rate of sub-ESOs and reduce the undesired chattering, but requires larger control inputs and energy consumption. Larger $\tilde{K}$ can improve the performance of attitude tracking and reduce undesired chattering, but will also require larger control inputs.

4.2 Desired angular velocity in square wave form

The attitude-tracking problem of a spacecraft with abrupt changes in the desired angular velocity is simulated in this subsection. Consider the desired angular velocity in the form

$$\omega_d(t) = [0.05, 0.03, 0.02]^{\mathrm{T}} \text{ rad/s}, \quad 2kT < t < (2k+1)T, \tag{54}$$

$$\omega_d(t) = -[0.05, 0.03, 0.02]^{\mathrm{T}} \text{ rad/s}, \quad (2k+1)T < t < (2k+2)T, \tag{55}$$

where $T = 10$ s is the switch period.

The parameters needed for two schemes, system initial states, ESO, and the event-triggering condition are all the same as described previously. Comparative-analysis results concerning the effects of uncertainties on the ET-ADRC scheme are summarized in Table 2. The simulation results of the ET-ADRC and CT-ADRC schemes with different average sampling periods T_A in terms of tracking errors E_v and E_q and QEC E_c are summarized in Table 3. The results of two schemes are shown in Figures 7–11. Similar to the simulation results of the previous subsection, the proposed ET-ADRC scheme achieves similar performances in terms of attitude quaternion and angular velocity tracking except at switch points (see Figures 8 and 9) and similar energy consumptions but with a lower sampling rate compared to the CT-ADRC scheme. Moreover, with the increase of average sampling times, the performance of the CT-ADRC

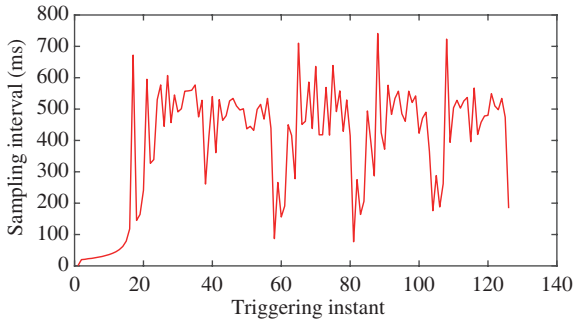

Figure 7 (Color online) Sampling intervals of ET-ADRC scheme with $\Psi = 2.5$ for square wave form.

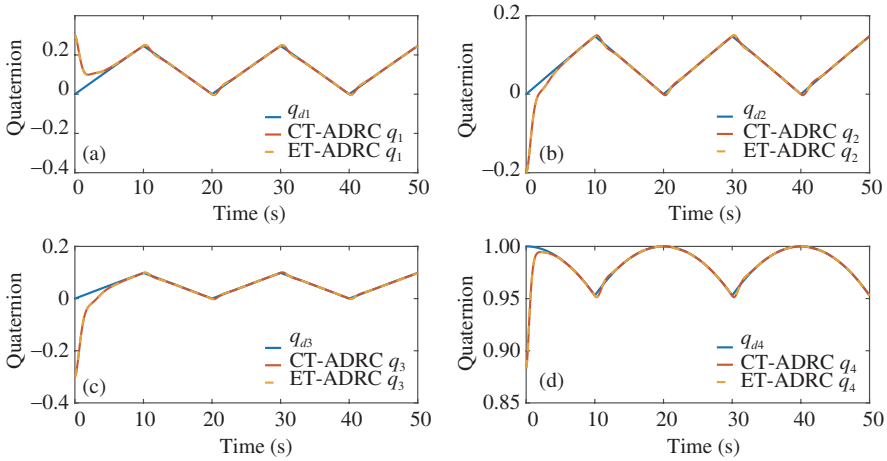

Figure 8 (Color online) Attitude quaternion tracking performance of square wave form. Tracking performance for (a) q_1, (b) q_2, (c) q_3, and (d) q_4.

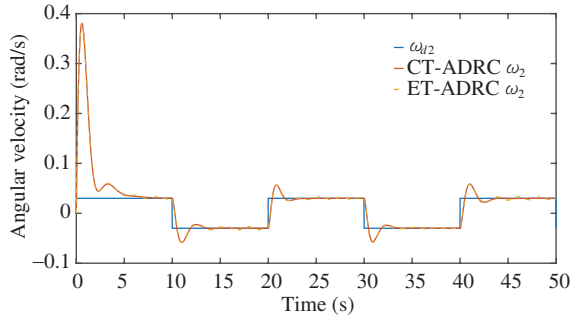

Figure 9 (Color online) Angular-velocity-tracking performance of square wave form.

scheme becomes worse than that of the ET-ADRC scheme (see Table 3); in particular, the ET-ADRC scheme achieves better angular-velocity-tracking performance but with lower sampling rates and energy consumption.

In general, we observe that, in comparison with the CT-ADRC scheme, the ET-ADRC scheme with two kinds of desired angular velocity can guarantee a similar performance in terms of tracking errors with a reduced average data-transmission rate.

5 Conclusion

Herein, the problem of attitude tracking with communication-resource restrictions has been investigated for spacecraft models with inertial uncertainties and external disturbances. Based on the proposed

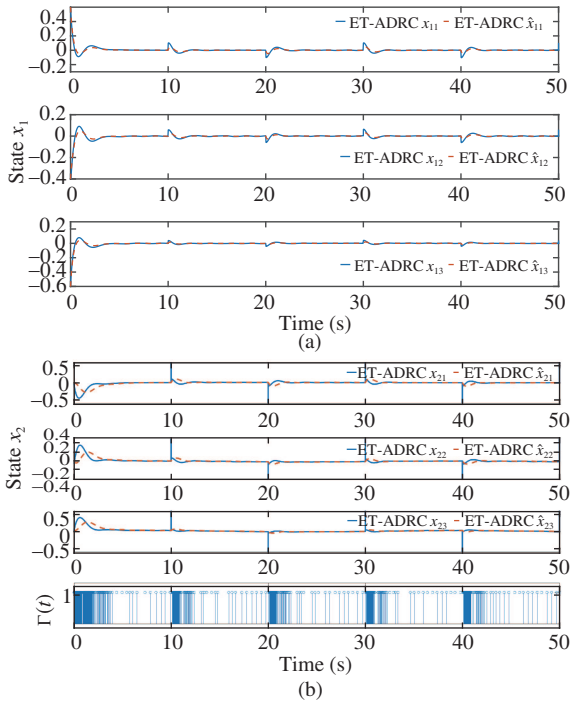

Figure 10 (Color online) Observation performance of ESO with event-triggered mechanism of square wave form. Observation performance for (a) x_1 and (b) x_2.

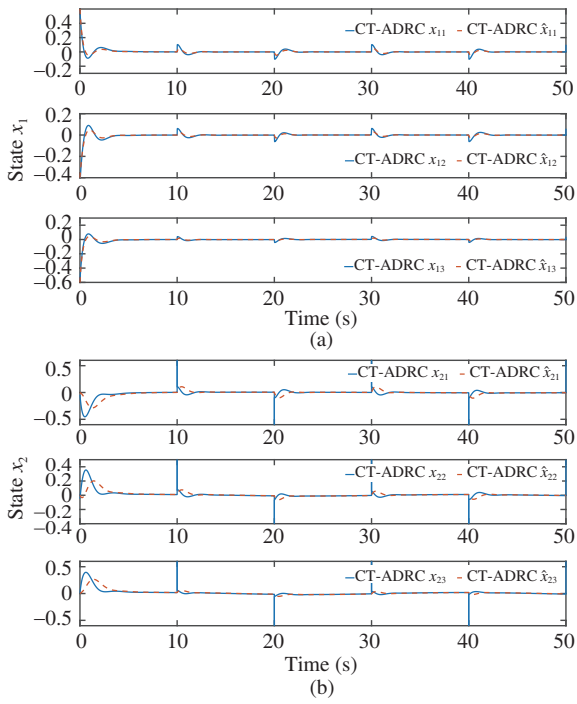

Figure 11 (Color online) Observation performance of ESO with time-triggered mechanism of square wave form. Observation performance for (a) x_1 and (b) x_2.

scheme, attitude tracking is achieved for a rigid spacecraft. An event-triggered mechanism is designed to guarantee the asymptotic boundedness of observation errors and the asymptotic stabilization of the attitude-tracking system. Simulation results with different kinds of desired angular velocity have been presented to illustrate the effectiveness of the developed method. As energy/fuel efficiency is important for spacecraft, event-triggered-controller design with explicit consideration of energy-consumption constraints is an interesting and relevant direction for future research, which will be considered in our next step.

Acknowledgements This work was supported by National Natural Science Foundation of China (Grant Nos. 61503027, 51675041). The authors would like to thank the associate editor and the anonymous reviewers for their suggestions which have improved the quality of the work.

References

1 Sidi M J. Spacecraft Dynamics and Control. Cambridge: Cambridge University Press, 2000
2 Crouch P. Spacecraft attitude control and stabilization: applications of geometric control theory to rigid body models. IEEE Trans Autom Control, 1984, 29: 321–331
3 Wang N, Zhang T W, Xu J Q. Formation control for networked spacecraft in deep space: with or without communication delays and with switching topology. Sci China Inf Sci, 2011, 54: 469–481
4 Jin Y Q, Liu X D, Qiu W, et al. Time-varying sliding mode control for a class of uncertain MIMO nonlinear system subject to control input constraint. Sci China Inf Sci, 2010, 53: 89–100
5 Pukdeboon C. Extended state observer-based third-order sliding mode finite-time attitude tracking controller for rigid spacecraft. Sci China Inf Sci, 2019, 62: 012206
6 Pukdeboon C, Zinober A S I, Thein M W L. Quasi-continuous higher order sliding-mode controllers for spacecraft-attitude-tracking maneuvers. IEEE Trans Ind Electron, 2010, 57: 1436–1444
7 Xia Y Q, Zhu Z, Fu M Y, et al. Attitude tracking of rigid spacecraft with bounded disturbances. IEEE Trans Ind Electron, 2011, 58: 647–659
8 Li Z K, Duan Z S. Distributed adaptive attitude synchronization of multiple spacecraft. Sci China Technol Sci, 2011, 54: 1992–1998
9 Chen Z Y, Huang J. Attitude tracking and disturbance rejection of rigid spacecraft by adaptive control. IEEE Trans Autom Control, 2009, 54: 600–605
10 Luo W C, Chu Y C, Ling K V. Inverse optimal adaptive control for attitude tracking of spacecraft. IEEE Trans Autom Control, 2005, 50: 1639–1654

11 Åström K J, Bo B. Comparison of periodic and event based sampling for first order stochastic systems. In: Proceedings of IFAC World Congress, Beijing, 1999. 5006–5011
12 Postoyan R, Bragagnolo M C, Galbrun E, et al. Event-triggered tracking control of unicycle mobile robots. Automatica, 2015, 52: 302–308
13 He N, Shi D W. Event-based robust sampled-data model predictive control: a non-monotonic Lyapunov function approach. IEEE Trans Circ Syst I, 2015, 62: 2555–2564
14 Huang N, Duan Z S, Zhao Y. Distributed consensus for multiple Euler-Lagrange systems: an event-triggered approach. Sci China Technol Sci, 2016, 59: 33–44
15 Yu Y G, Zeng Z W, Li Z K, et al. Event-triggered encirclement control of multi-agent systems with bearing rigidity. Sci China Inf Sci, 2017, 60: 110203
16 Sun S, Yang M F, Wang L. Event-triggered nonlinear attitude control for a rigid spacecraft. In: Proceedings of the 36th Chinese Control Conference, 2017. 7582–7586
17 Xing L T, Wen C Y, Liu Z T, et al. An event-triggered design scheme for spacecraft attitude control. In: Proceedings of IEEE Conference on Industrial Electronics and Applications, 2017. 1552–1557
18 Wu B L, Shen Q, Cao X B. Event-triggered attitude control of spacecraft. Adv Space Res, 2018, 61: 927–934
19 Zhang C X, Wang J H, Zhang D X, et al. Learning observer based and event-triggered control to spacecraft against actuator faults. Aerosp Sci Tech, 2018, 78: 522–530
20 Han J Q. From PID to active disturbance rejection control. IEEE Trans Ind Electron, 2009, 56: 900–906
21 Zheng Q, Gao Z Q. On practical applications of active disturbance rejection control. In: Proceedings of the 29th Chinese Control Conference, 2010. 6095–6100
22 Guo B Z, Wu Z H, Zhou H C. Active disturbance rejection control approach to output-feedback stabilization of a class of uncertain nonlinear systems subject to stochastic disturbance. IEEE Trans Autom Control, 2016, 61: 1613–1618
23 Li S L, Yang X, Yang D. Active disturbance rejection control for high pointing accuracy and rotation speed. Automatica, 2009, 45: 1854–1860
24 Sira-Ramírez H, Linares-Flores J, García-Rodríguez C, et al. On the control of the permanent magnet synchronous motor: an active disturbance rejection control approach. IEEE Trans Control Syst Technol, 2014, 22: 2056–2063
25 Tang S, Yang Q H, Qian S K, et al. Height and attitude active disturbance rejection controller design of a small-scale helicopter. Sci China Inf Sci, 2015, 58: 032202
26 Chen S, Xue W C, Zhong S, et al. On comparison of modified ADRCs for nonlinear uncertain systems with time delay. Sci China Inf Sci, 2018, 61: 070223
27 Huang Y, Wang J Z, Shi D W, et al. Toward event-triggered extended state observer. IEEE Trans Autom Control, 2018, 63: 1842–1849
28 Shi D W, Xue J, Zhao L X, et al. Event-triggered active disturbance rejection control of DC torque motors. IEEE/ASME Trans Mechatron, 2017, 22: 2277–2287
29 Yuan J S. Closed-loop manipulator control using quaternion feedback. IEEE J Robot Autom, 1988, 4: 434–440
30 Lu K F, Xia Y Q, Fu M Y. Controller design for rigid spacecraft attitude tracking with actuator saturation. Inf Sci, 2013, 220: 343–366
31 Yang H J, You X, Xia Y Q, et al. Adaptive control for attitude synchronisation of spacecraft formation via extended state observer. IET Control Theory Appl, 2014, 8: 2171–2185
32 Guo B Z, Zhao Z L. On convergence of nonlinear active disturbance rejection for SISO systems. In: Proceedings of the 24th Chinese Control and Decision Conference, 2012. 3507–3512
33 Bai W Y, Xue W C, Huang Y, et al. On extended state based Kalman filter design for a class of nonlinear time-varying uncertain systems. Sci China Inf Sci, 2018, 61: 042201
34 Li B, Hu Q L, Ma G F. Extended state observer based robust attitude control of spacecraft with input saturation. Aerospace Sci Tech, 2016, 50: 173–182
35 Li B, Hu Q L, Yu Y B, et al. Observer-based fault-tolerant attitude control for rigid spacecraft. IEEE Trans Aerosp Electron Syst, 2017, 53: 2572–2582
36 Cai D H, Zou H G, Wang J Z, et al. Supplementary discussions on "event-triggered attitude tracking for rigid spacecraft". 2019. http://www.escience.cn/people/dshi/
37 Khalil H K. Nonlinear Systems. Englewood Cliffs: Prentice Hall, 2002
38 Li P, Yue X K, Chi X B, et al. Optimal relative attitude tracking control for spacecraft proximity operation. In: Proceedings of the 25th Chinese Control and Decision Conference, 2013